

# Revisiting Fracture via the Multiscale Scaled Boundary Finite Element Method

Adrian Egger <[egger@ibk.baug.ethz.ch](mailto:egger@ibk.baug.ethz.ch)>



**1 Motivation****2 SBFEM**

- Discretization
- Equation
- Solution
- Stress intensity factors

**3 Extended Multiscale Finite Element Method****4 Quadtree based multiscale SBFEM analysis****5 Example**

- Introduction
- RVE
- Masonry Wall
- Hybrid BC

**6 Conclusions****7 Thanks**

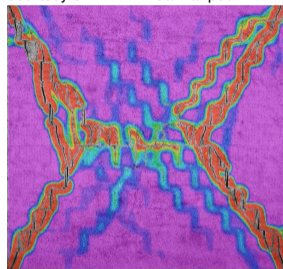
Many contemporary structural engineering problems are inherently **multiscale** in nature:

- Numerical simulation of masonry walls
- Fatigue assessment of wind turbine blades

The **SBFEM** is (1) highly efficient and (2) flexible, featuring a semi-analytical solution that introduces many advantages:

- 1 Egger et al. (2017), A robust and efficient SBFEM [...], Arch. of Appl. Mech.
- 2 Ooi et al. (2015), Adaptation of quadtree meshes [...], Eng. Fract. Mech.

courtesy of Dr. Amir Salmanpour



<https://www.wind-watch.org>



Motivation

SBFEM

Discretization

Equation

Solution

SIFs

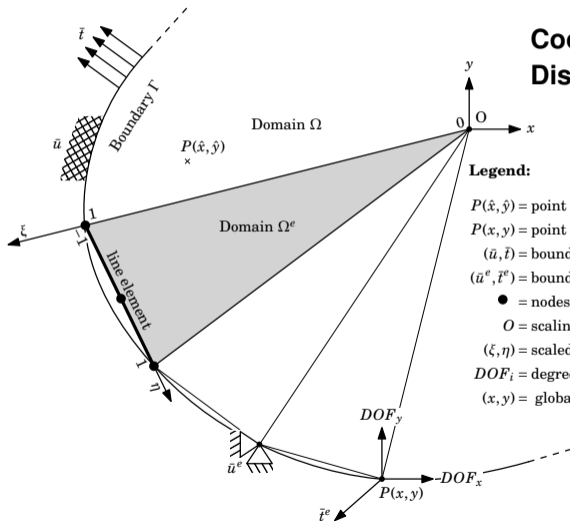
EMsFEM

qtMSBFEM

Example

Conclusions

Thanks

Coordinates:  $x(\xi, \eta) = x_0 + \xi [N(\eta)] \{x\}$ Displacements:  $u(\xi, \eta) = [N^u(\eta)] \{u(\xi)\}$ **Legend:** $P(\hat{x}, \hat{y})$  = point in domain $P(x, y)$  = point on boundary $(\bar{u}, \bar{i})$  = boundary conditions of domain $(\bar{u}^e, \bar{i}^e)$  = boundary conditions of elements (i.e. discretized boundary)● = nodes of line element with coordinates  $(x_n, y_n)$  $O$  = scaling center and origin of normalized radial coordinate  $\xi$  $(\xi, \eta)$  = scaled boundary coordinates with  $0 \leq \xi \leq 1$  and  $-1 \leq \eta \leq 1$ DOF<sub>*i*</sub> = degree of freedom of each node in global  $(x, y)$ -direction $(x, y)$  = global coordinate system

Upon application of the principle of virtual work two equations arise. The first is valid only on the boundary, while the **second term** holds for the domain and is termed **the scaled boundary finite element equation**:

$$\{P\} = [E^0]\{u\}_{,\xi} + [E^1]^T\{u\} \quad (1)$$

$$[E^0]\xi^2\{u(\xi)\}_{,\xi\xi} + [[E^0] + [E^1]^T - [E^1]]\xi\{u(\xi)\}_{,\xi} - [E^2]\{u(\xi)\} = \{0\} \quad (2)$$

with the following substitutions:

$$[E^0] = \int_{\partial\Omega} [B^1(\eta)]^T [D] [B^1(\eta)] |J| d\eta \quad (3a)$$

$$[E^1] = \int_{\partial\Omega} [B^1(\eta)]^T [D] [B^2(\eta)] |J| d\eta \quad (3b)$$

$$[E^2] = \int_{\partial\Omega} [B^2(\eta)]^T [D] [B^2(\eta)] |J| d\eta \quad (3c)$$

Assuming the **general solution as a power series**, we can rewrite the previous equations in modal form:

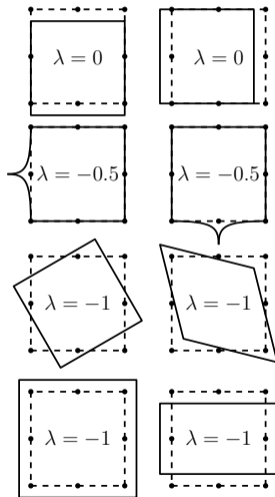
$$\{u(\xi)\} = [\phi]\xi^{[-\lambda]}\{c\} \quad (4)$$

such that (1) and (2) may be more compactly rewritten as:

$$[Z] \begin{Bmatrix} \phi \\ q \end{Bmatrix} = [\lambda] \begin{Bmatrix} \phi \\ q \end{Bmatrix} = \begin{bmatrix} \lambda_- & \\ & \lambda_+ \end{bmatrix} \begin{bmatrix} [\phi_1] & [\phi_2] \\ [Q_1] & [Q_2] \end{bmatrix} \quad (5)$$

with the **Hamiltonian matrix Z** given as:

$$[Z] = \begin{bmatrix} [E^0]^{-1}[E^1]^T & -[E^0]^{-1} \\ [E^1][E^0]^{-1}[E^1]^T - [E^2] & -[E^1][E^0]^{-1} \end{bmatrix} \quad (6)$$



Retaining the bounded response corresponding to the negative eigenvalues:

$$\{u(\xi)\} = [\phi_1] \xi^{[-\lambda_-]} \{c_1\} \quad (7)$$

and thus on the boundary ( $\xi = 1$ ) after rearranging:

$$\{c_1\} = [\Phi_1]^{-1} \{u(\xi = 1)\} \quad (8)$$

By equation to the modal representation of the external forces on the boundary:

$$\{P_{bounded}\} = [q_1] \{c_1\} = [q_1][\Phi_1]^{-1} \{u(\xi = 1)\} = \mathbf{K}_{bounded} \{u(\xi = 1)\} \quad (9)$$

The stiffness matrix  $\mathbf{K}_{bounded}$ , though **fully populated**, is **symmetric** and only of dimension  $nDOF_{boundary}$ .

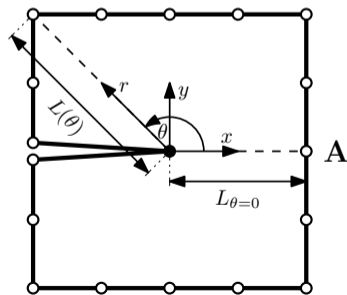
By inspection of the general solution, the **singular modes**, corresponding to the range of eigenvalues  $-1 < \lambda_s < 0$ , are identified.

Consequently, an expression of the **singular stresses** follows as<sup>1</sup>:

$$\{\sigma^s(\xi, \eta)\} = [D](-\lambda_s[B^1] + [B^2])[\phi_s]\xi^{-[\lambda]-[1]}\{c^s\} \quad (10)$$

Assuming a **square root type singularity**, the stress intensity factors are obtained by substitution of the numerically obtained singular stresses into their formal definition:

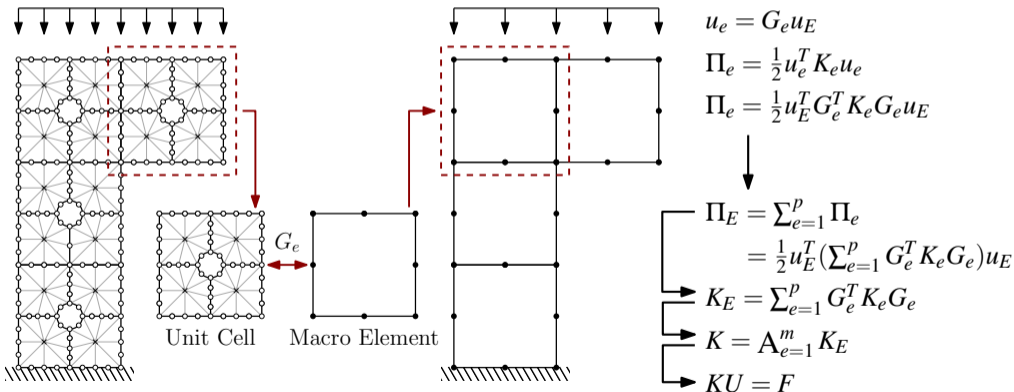
$$\begin{Bmatrix} K_I \\ K_{II} \end{Bmatrix} = \sqrt{2\pi L_0} \begin{Bmatrix} \sum\{\sigma_{yy}^s(\xi=1, \eta=\eta_A)\}\{c^s\} \\ \sum\{\sigma_{xy}^s(\xi=1, \eta=\eta_A)\}\{c^s\} \end{Bmatrix}$$



<sup>1</sup> <https://doi.org/10.1007/s00419-017-1280-7>

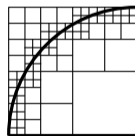
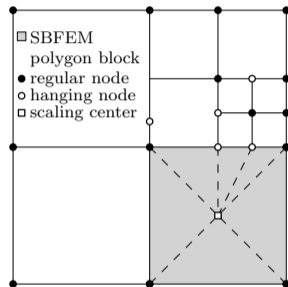


**Numerical basis functions (NBF),  $G_i$** , map the response between the fine (e-micro) and coarse (E-macro) mesh, while maintaining **energy equivalence**.

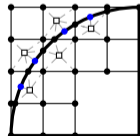


SBFEM and quadtree type decompositions complement each other:

- **Complex geometries** such as inclusions and discontinuities are easily and efficiently meshed
- **No hanging node** issues
- **Precomputation** of stiffness matrices
- Irregular shapes (curves) considered via **higher order SBFEM elements**
- Control over boundary discretization beneficial for constructing numerical basis functions
- Permits use of **oversampling**

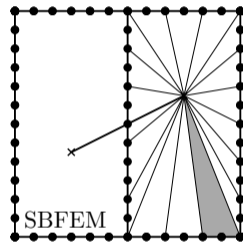
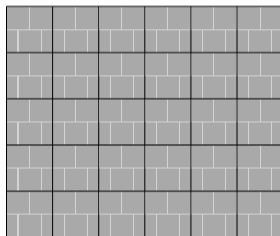
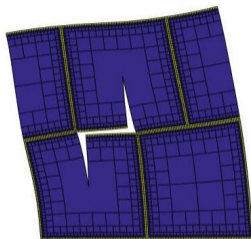


FEM



SBFEM

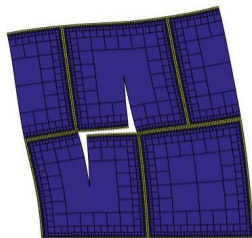
Influence of the amount of coarse nodes on the accuracy of the solution for RVE's containing large discontinuities and their corresponding SIFs.



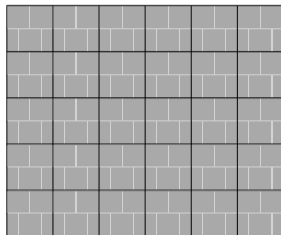
- Cracked domain
- Abaqus (reference), SBFEM, MSBFEM
- $\|u_h - u_{ref}\|_2 / \|u_{ref}\|_2$
- SIFs

- SBFEM vs MSBFEM
- plots  $u_h^{magn.}$  and  $\sigma_h^{mises}$
- $\|u_h - u_{ref}\|_2 / \|u_{ref}\|_2$
- Computational savings

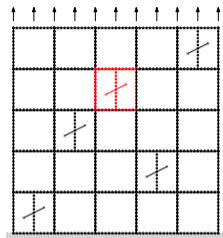
- Hybrid BC
- Higher order elements
- SIFs



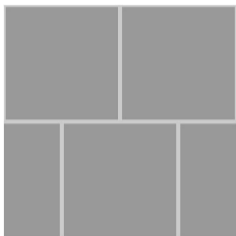
- Fully restrained base
- Top surface load: shear & tension,  $q = 0.1$
- $E_{mod}^{bri} = 11$ ,  $E_{mod}^{mor} = 7$ ,  $\nu_j = 0.25$
- side length  $l = 512$



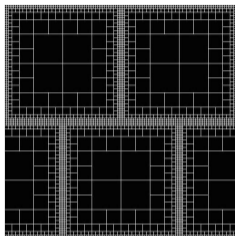
- Fully restrained base
- Top surface BC:  $y = 0$
- Top surface load: shear  $q = 0.1$
- $E_{mod}^{bri} = 11$ ,  $E_{mod}^{mor} = 7$ ,  $\nu_j = 0.25$



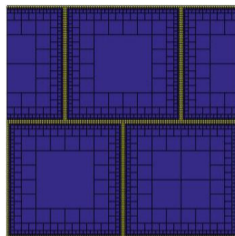
- Isotrop. domain
- Embedded in wall assembly
- $E = 200$ ,  $\nu = 0.25$
- varying a/L ratio



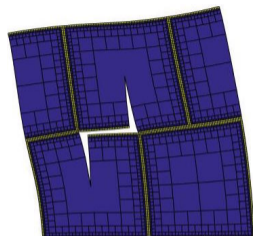
**Step 1:**  
Definition of RVE can be as easy as taking a photograph



**Step 2:**  
The domain is partitioned into blocks by quadtree decomposition



**Step 3:**  
Each block represents an SBFEM polygon element and is then assembled



**Step 4:**  
Double nodes are inserted to create crack seams. Blocks are merged to position the crack tip.

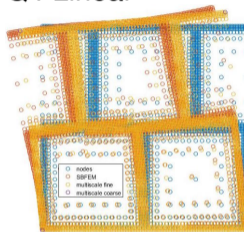
## Error in displacement norms:

#cNodes	Linear	Periodic
<b>Q4</b>	$331 \cdot 10^{-3}$	$324 \cdot 10^{-3}$
<b>Q8</b>	$118 \cdot 10^{-3}$	$102 \cdot 10^{-3}$
<b>Q12</b>	$38 \cdot 10^{-3}$	$170 \cdot 10^{-3}$
<b>Q16</b>	$16 \cdot 10^{-3}$	$192 \cdot 10^{-3}$
<b>SBFEM</b>	$428 \cdot 10^{-5}$	-

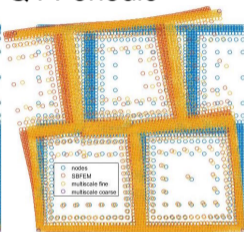
## Observations:

For higher noded coarse elements, periodic BC underperform. Oscillatory behavior does not mimic the structural response when discontinuities are present in domain.

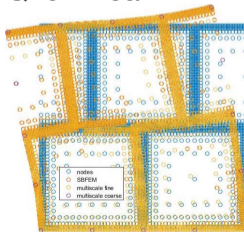
### Q4 Linear



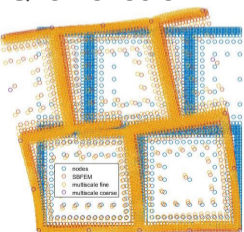
### Q4 Periodic



### Q16 Linear



### Q16 Periodic



## Top crack tip

		Linear			
2-N	K1	%Err	K2	%Err	
Q4	0.925	55.7	1.716	51.9	
Q8	1.296	37.9	2.605	27.0	
Q12	1.692	19.0	3.251	8.9	
Q16	1.864	10.7	3.281	8.1	
SBFEM	1.982	5.1	3.356	6.0	
Abaqus	2.088	-	3.569	-	

		periodic			
2-N	K1	%Err	K2	%Err	
Q4	0.971	53.5	2.245	37.1	
Q8	1.584	24.1	2.518	29.4	
Q12	1.762	15.6	3.284	8.0	
Q16	1.830	12.4	3.336	6.5	

## Lower crack tip

		Linear			
2-N	K1	%Err	K2	%Err	
Q4	1.271	8.0	2.059	26.4	
Q8	1.383	-0.1	1.941	30.6	
Q12	1.149	16.9	2.334	16.6	
Q16	1.288	6.8	2.547	9.0	
SBFEM	1.306	5.5	2.633	5.9	
Abaqus	1.382	-	2.797	-	

		periodic			
2-N	K1	%Err	K2	%Err	
Q4	0.898	35.0	2.037	27.2	
Q8	0.745	46.1	2.461	12.0	
Q12	0.623	54.9	2.848	-1.8	
Q16	0.886	35.9	2.840	-1.5	

		Linear			
3-N	K1	%Err	K2	%Err	
Q4	0.956	54.2	1.803	49.5	
Q8	1.345	35.6	2.735	23.4	
Q12	1.760	15.7	3.424	4.1	
Q16	1.944	6.9	3.456	3.2	
SBFEM	2.069	0.9	3.539	0.9	

		periodic			
3-N	K1	%Err	K2	%Err	
Q4	1.008	51.7	2.364	33.7	
Q8	1.649	21.0	2.655	25.6	
Q12	1.837	12.0	3.464	2.9	
Q16	1.907	8.7	3.518	1.4	

		Linear			
3-N	K1	%Err	K2	%Err	
Q4	1.327	4.0	2.153	23.0	
Q8	1.456	-5.3	2.037	27.2	
Q12	1.204	12.8	2.455	12.2	
Q16	1.352	2.1	2.682	4.1	
SBFEM	1.370	0.9	2.776	0.8	

		periodic			
3-N	K1	%Err	K2	%Err	
Q4	0.941	31.9	2.145	23.3	
Q8	0.783	43.3	2.594	7.2	
Q12	0.649	53.0	3.005	-7.4	
Q16	0.927	33.0	2.997	-7.2	

## Annotations:

Reference SIFs (Abaqus) computed via contour integral and quadratic elements, nodes at quarter points, and contrasted to SBFEM & MSBFEM, with the cracked domain modeled by 2-noded (2-N) or 3-noded elements (3-N).

## Performance comparison:

- Reduction of overall DOF
- Reduction of computational time
- Computational cost of offline NBF stage
- Effect on error norm of displacements

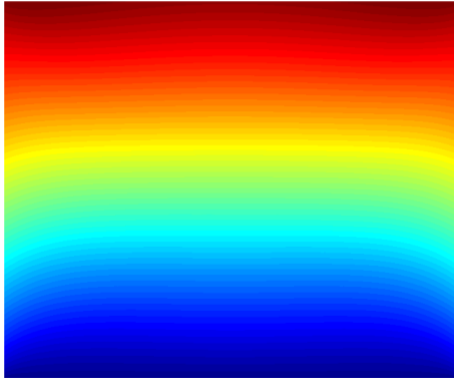
## Notes:

- Periodic BC more expensive, requires lagrange multipliers
- Linear BC offer better error norms for Q8 - Q16
- Large error norms for periodic BC
  - Oscillatory behavior violates global BC
  - Superior in approximating interior displacements and stresses though

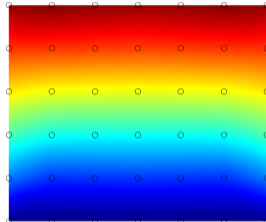
	Q4		Q8		Q12		Q16		Units
	L	P	L	P	L	P	L	P	
DOF SBFEM	96189		96189		96189		96189		-
DOF MSBFEM	84		226		368		510		-
Ratio	11451		4256		2614		1886		x
Time SBFEM	0.6247		0.6247		0.6247		0.6247		[s]
Time MSBFEM	0.0008		0.0026		0.0028		0.0048		[s]
Ratio	762		243		227		131		x
Time NBF	0.667	0.700	1.027	1.325	1.537	1.894	1.862	2.534	[s]
Displ. Norm	34.54	28.83	3.65	65.06	1.86	46.57	1.31	43.37	-



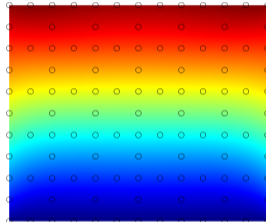
**SBFEM reference:**



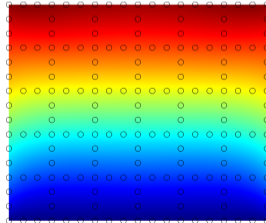
**Q4:**



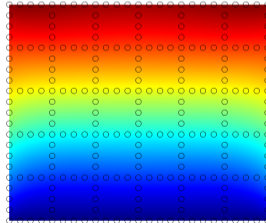
**Q8:**



**Q12:**



**Q16:**



Motivation

SBFEM

EMsFEM

qtMSBFEM

**Example**

Introduction

RVE

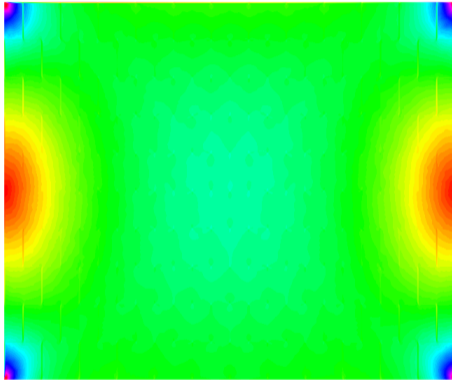
Masonry Wall

Hybrid BC

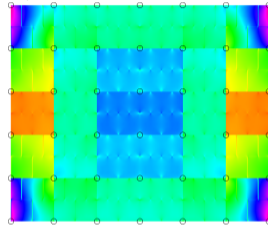
Conclusions

Thanks

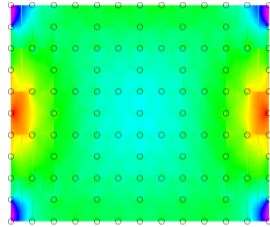
SBFEM reference:



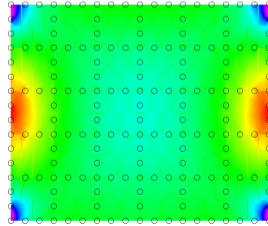
Q4:



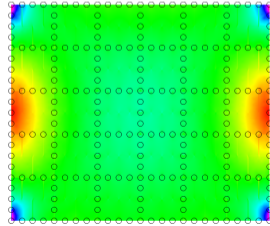
Q8:



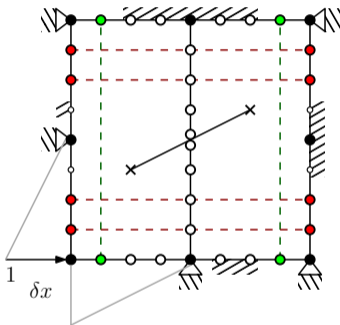
Q12:



Q16:



## Hybrid BC scheme for NBF



a/L	Q4						Q8					
	Linear		Periodic		Hybrid		Linear		Periodic		Hybrid	
	K1	K2	K1	K2	K1	K2	K1	K2	K1	K2	K1	K2
0.45	29.00	32.66	20.57	15.24	21.83	17.85	8.27	24.17	10.24	1.56	8.57	4.95
0.40	23.10	27.54	13.93	17.78	15.31	19.24	5.03	16.35	12.76	1.66	6.19	3.86
0.35	18.46	23.19	9.43	19.62	10.79	20.16	2.13	10.89	12.29	0.75	3.66	2.27
0.30	14.50	18.96	6.48	19.21	7.68	18.99	0.41	7.45	10.16	0.18	1.87	1.27
0.25	10.91	14.67	4.39	16.44	5.37	14.94	2.51	5.76	7.52	0.12	3.26	0.96
0.20	7.55	10.42	2.76	12.22	3.48	10.69	4.17	5.38	4.99	0.21	4.29	0.99
0.15	4.51	6.43	1.47	7.65	1.92	6.61	5.43	5.96	2.82	0.21	3.21	1.07
0.10	2.03	3.06	0.53	3.63	0.76	3.15	6.20	7.19	1.14	0.09	1.90	1.15
0.05	0.42	0.85	0.02	0.96	0.08	0.87	5.72	8.91	0.09	0.05	0.94	1.38

a/L	Q12						Q16					
	Linear		Periodic		Hybrid		Linear		Periodic		Hybrid	
	K1	K2	K1	K2	K1	K2	K1	K2	K1	K2	K1	K2
0.45	4.50	1.82	8.77	0.89	5.14	1.03	0.60	5.07	4.09	3.03	1.12	3.34
0.40	1.63	0.21	8.92	0.93	2.72	0.32	0.05	3.66	4.79	3.75	0.76	3.67
0.35	0.73	0.42	8.01	0.69	1.82	0.46	0.54	2.15	4.75	2.85	1.17	2.25
0.30	0.63	0.75	6.26	0.08	1.47	0.18	0.58	1.10	4.02	1.70	1.10	1.19
0.25	0.63	0.84	4.36	0.24	1.19	0.33	0.44	0.54	3.03	0.91	0.83	0.60
0.20	0.54	0.73	2.73	0.30	0.87	0.36	0.28	0.28	2.04	0.47	0.55	0.31
0.15	0.36	0.49	1.45	0.25	0.52	0.29	0.16	0.15	1.17	0.21	0.31	0.16
0.10	0.17	0.25	0.53	0.18	0.23	0.19	0.07	0.08	0.49	0.04	0.13	0.05
0.05	0.04	0.07	0.03	0.12	0.03	0.07	0.01	0.04	0.05	0.07	0.02	0.04

**Benefits:** Better representation of displacements and overall strain within domain. More consistent characterization of SIFs. Benefits of periodic BC, where applicable, while considering physical crack behavior.

## Positive:

- Fusion of quadtree decomp., SBFEM and EMsFEM concepts
- Significant computational savings
- Accurately capture SIFs
- Hybrid BC proposed

## Negative:

- Increased program complexity
- NBF computationally intensive, but an offline calculation and embarrassingly parallel
- NBF computational toll recovered only for time dependent problems

## Outlook:

- Quadtree decomposition with higher order elements
- Behaviour when cracks extend across RVE boundaries
- Multiple cracks in same problem domain

This research was performed under the auspices of the **Swiss National Science Foundation (SNSF), Grant # 200021 153379**, A Multiscale Hysteretic XFEM Scheme for the Analysis of Composite Structures

Further, we would like to extend our gratitude to **Prof. Dr. Chongmin Song** (UNSW) as well as **Dr. Konstantinos Agathos** (ETHZ) for their insightful discussions.